Available online at www.eccomasproceedia.org
Eccomas Proceedia COMPDYN (2019) 4968-4983

ECCOMAS
Proceedia

COMPDYN 2019
7th ECCOMAS Thematic Conference on
Computational Methods in Structural Dynamics and Earthquake Engineering
M. Papadrakakis, M. Fragiadakis (eds.)
Crete, Greece, 24–26 June 2019

USING DIRECT ECONOMIC LOSSES AND COLLAPSE RISK FOR SEISMIC DESIGN OF RC BUILDINGS

Davit Shahnazaryan[1], Gerard J. O'Reilly[1], Ricardo Monteiro[1]

[1] Scuola Universitaria Superiore IUSS Pavia
Palazzo del Broletto, Piazza della Vittoria 15, Pavia 27100, Italy
e-mail: {davit.shahnazaryan,gerard.oreilly,ricardo.monteiro}@iusspavia.it

Abstract

In recent years, the consideration of earthquake-induced expected annual loss (EAL) has become a topic of great interest within the earthquake engineering community. Since the introduction of performance-based earthquake engineering (PBEE) in the 1990s, the principal goal of seismic design has been the verification of limit states in addition to the use of meaningful metrics of seismic performance that respond to the diverse needs and objectives of owner-users and society. However, the need for more focus on the control of earthquake-induced losses at a design stage is also of importance and interest. One possible solution for this gap may be to use a conceptual design framework that employs EAL as a design metric, serving as a first design step to identify suitable typologies and geometrical layouts. The objective of such an approach, which would require very little building information at the design outset, is to identify a number of feasible building typologies, in terms of lateral force resisting system, and associated structural geometries. This study implemented such a novel EAL-based design methodology, recently proposed, for a reinforced concrete (RC) frame as a parametric case study within the European context. A sensitivity study on the use of storey loss functions was also done to identify their compatibility with and impact on the framework at different performance limit states. Furthermore, effectively controlling the structure's ultimate limit state whilst also arriving at practical design solutions was seen to be an issue that requires further development. An alternative method to control collapse risk during design whilst also maintaining control on the EAL of the structure was therefore identified. As such, a conceptual design framework that focuses on both the economic losses and life safety in a direct and quantifiable manner has been identified to further implement the principles of PBEE in design practice.

Keywords: Performance-Based Earthquake Engineering; Conceptual Design; Reinforced Concrete; Expected Annual Loss; Storey Loss Functions.

ISSN:2623-3347
Peer-review under responsibility of the organizing committee of COMPDYN 2019.
doi: 10.7712/120119.7281.19516

1 INTRODUCTION

Current seismic design guidelines have a two-fold performance objective: the protection of human lives and the limitation of earthquake-induced damage. Hence, it is important to limit the likelihood of structural collapse, which is obtained by providing sufficient strength and ductility, in addition to proper detailing and capacity design, ensuring a controlled and stable ductile mechanism during strong seismic shaking. Additionally, damage limitation can be controlled during more frequent events. Neglecting damage control at a design stage can have severe consequences during an earthquake as both structural and non-structural damage, in conjunction with the interruption of building use, may entail disproportionally high economical losses compared to the costs of the structure itself. These aspects partially form what has become known as the Pacific Earthquake Engineering Research (PEER) PBEE methodology initially outlined by Cornell and Krawinkler [1]. This PBEE methodology [2,3] is an approach to quantify the performance of a given structural system. It utilises a fully probabilistic framework, employing methodologies with a solid scientific basis to improve seismic risk decision-making and expresses the levels of performance in terms of metrics meaningful to stakeholders and building owners. New guidelines like FEMA P58 [4] were developed, which allow the performance of existing buildings to be quantified in terms of metrics like expected annual loss (EAL) and mean annual frequency of collapse (MAFC). However, due to its iterative and cumbersome nature, more simplified options to take EAL into account have been sought.

O'Reilly and Calvi [5] recently proposed a novel conceptual seismic design (CSD) framework that employs EAL as a design metric and requires very little building information at the design onset. The framework encompasses the idea that designers may start with the definition of a required or limiting value of EAL and arrive at a number of feasible structural solutions without the need for any detailed design calculations or numerical analysis. Initially, the building performance definition is transformed into a design solution space using a number of simplifying assumptions. Subsequently, with a suitable structural response backbone, a number of feasible building typologies and associated structural geometries are identified. It is important to note that the methodology forms a stepping stone prior to further member detailing and robust design verifications, such as that outlined in FEMA P58.

This study aims to describe a detailed implementation of the CSD framework [5] and provide further insight by means of a parametric study. Serviceability limit state parameters are initially varied to see their effect on the design EAL and an alteration of the design solution space. A study on the use of storey loss functions (SLFs) is then carried out for their modification to overcome their incompatibility with the CSD framework at the ultimate limit state, in view of it not affecting the EAL. Finally, an approach to consider target collapse safety to define prospective structure's dynamic and strength characteristics is discussed, which could potentially solve the issues identified during the sensitivity study on SLFs.

2 CONCEPTUAL SEISMIC DESIGN

In order to implement the CSD framework shown in Figure 1, some simplifying assumptions are needed initially. First, SLFs are used to convert expected loss ratios (ELRs) to design peak storey drift (PSD) and peak floor acceleration (PFA). Three limit states were utilised: fully operational limit state (OLS); serviceability limit state (SLS); and ultimate limit state (ULS). Two limit state intensities, SLS and ULS, are considered to characterise the structure's elastic and ductile non-linear behaviour, respectively. The OLS performance point

describes the point when direct monetary losses begin to accumulate due to building damage, which can be thought of as an initial threshold akin to the excess amount on an insurance policy. The ULS performance point describes the point of building's full monetary replacement cost (Figure 3).

Current codes define the seismic design problem primarily in terms of ensuring life safety of its occupants. Therefore, mitigation of collapse is of primary importance and ensuring satisfactory performance at frequent levels of shaking is also checked. These are termed as '*no-collapse requirement*' and '*damage limitation requirement*' in the current version of Eurocode 8 (EC8) [6] and are suggested to correspond to ground shaking return periods of 475 and 95 years, respectively, with possible modifications to account for building importance class. New Zealand's NZS1170 [7] defines two limit states: serviceability and ultimate similar to EC8 and prescribes design return periods of 25 and 500 years, respectively, once again with the possibility of modification for different importance classes. The recently revised design code in the US, ASCE 7-16 [8], outlines a slightly modified approach where the building is designed using input as a fraction of the maximum considered event (MCE). The seismic hazard is determined from a series of maps outlining risk-targeted spectral values, which are found for a target risk of structural collapse of 1% in 50 years (~5,000 year return period). It uses a generic structural fragility curve along with some other adjustments following an approach outlined by Luco *et al.* [9] but has recently been noted by Vamvatsikos [10] to perhaps not be the most ideal approach. In this study, these general recommendations provided above for the definition of limit state return period will be followed for the case study application in Section 3 and parametric studies in Section 4.1.

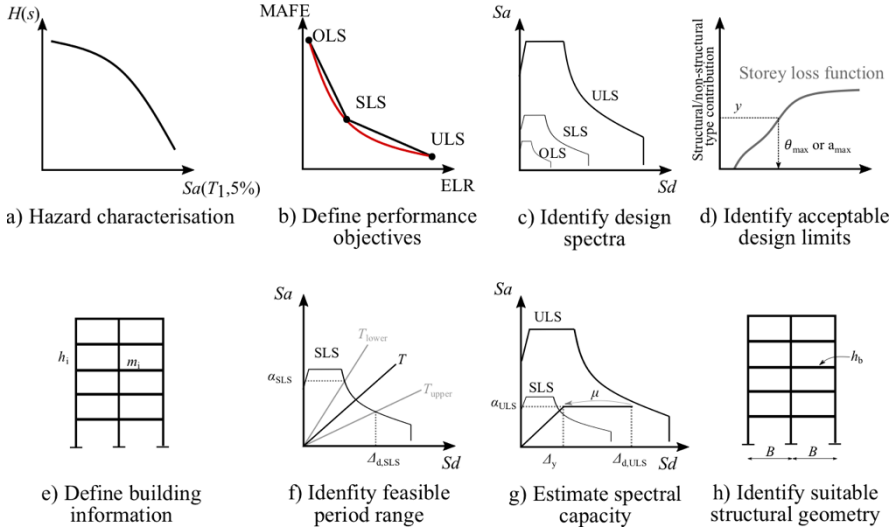

Figure 1: Overview of CSD framework for RC frames [5].

The CSD framework [5] is separated into two distinct parts: the identification of performance requirements, and the identification of feasible structural solutions. An overview of the framework for an RC frame is described in Figure 1. The first part includes: a) the site hazard initially identified with a uniform hazard spectra (UHS) for different return periods; b) performance objectives are set to establish the design loss curve characterised by an expected loss ratio (ELR, y), and corresponding mean annual frequency of exceedance (MAFE, λ), for each limit state. The loss curve is then integrated for the definition of design EAL, which has to be met by the subsequent obtainment of design solutions (Figure 3); c) using the MAFE for each limit state and the return periods of the UHS to be designed for, design spectra are identified; d) with the identification of design spectra, SLFs are used to relate expected monetary

losses to design parameters like the maximum PSD, θ_{max}, and maximum PFA, a_{max}, along the height of the building. The vertical axis in Figure 1(d) represents the ELR, y, contribution from PSD or PFA sensitive structural or non-structural elements.

The second part includes the following steps: e) minimal building information is needed, such as the number of storeys, n, seismic mass, m_i, and storey heights, h_i; f) at SLS, θ_{max} and a_{max} are converted to spectral displacement and acceleration limits, $\Delta_{d,SLS}$ and α_{SLS}, respectively. These are then used to identify the feasible initial secant to yield period range, where the initial period, T_1, of the sought structure must lie; g) knowing the design displacement at ULS, $\Delta_{d,ULS}$, and the required ductility, μ, the bilinear backbone curve is identified; h) and finally a suitable structural geometry from the established yield displacement, Δ_y, knowing that the yield displacement is a function of structural geometry and material properties. In the case of RC frames, the bay width, B, and the beam height, h_b, are computed. Overall, the framework works as an initial screening for suitable design before detailing and verification of the structure.

3 CASE STUDY APPLICATION

The CSD framework summarised in the previous section was used for a case study application herein. The goal of the study was to define certain performance objectives and come up with a set of design solutions in terms of bilinear backbone behaviour and required structural dimensions. No detailed verification analysis of these designs was carried out. Reasonable assumptions were made during the design process, since some information was not readily available. Minimal building information was necessary to implement the CSD framework. For the case study building discussed herein, a four-storey building with a floor area of 200m^2, seismic floor loading of 8kPa and roof loading of 7kPa was considered. The storey height was taken as 3.5m. The target EAL for the case study RC frame was predefined as 0.7%. With the already identified building performance requirements and minimal global characteristics of the possible building, a number of feasible design solutions were identified.

3.1 Identify site hazard

For the first step, the site hazard curve, H, was identified. Peak ground acceleration (PGA) was adopted along with EC8's type 1 design spectrum and soil type C was assumed. A higher fidelity second-order hazard model [11] was adopted instead of the first-order model initially utilised by O'Reilly and Calvi [5] to give a more accurate representation of the hazard, as described by Equation 1:

$$H(s) = k_0 \exp\left(-k_2 \ln^2 s - k_1 \ln s\right) \tag{1}$$

where the coefficients k_o, k_1 and k_2 were found to be 4.61E-05, 2.384 and 0.169, respectively, via a least-squares regression of the SHARE model [12] for a site in L'Aquila, Italy; and $H(s)$ is the hazard function representing the MAFE of a certain IM value s equal to PGA (Figure 2).

3.2 Define building performance objectives

Design performance objectives for the case study building are identified in Table 1. The values of return period, T_R, and ELR are decided. Then $H=1/T_R$ is used to determine the MAFE from Equation 2:

$$\lambda = \sqrt{p} k_0^{1-p} \left[H\left(\hat{s}\right)^p \right] \exp\left(\frac{1}{2} p k_1^2 \beta_s^2 \right)$$
$$p = \frac{1}{1 + 2k_2 \beta_s^2} \tag{2}$$

where $\hat{s}$ is the median value of s for a given limit state exceedance. Through the integration of the refined loss curve of Figure 3 and Equation 3, the EAL is computed and verified against the target one.

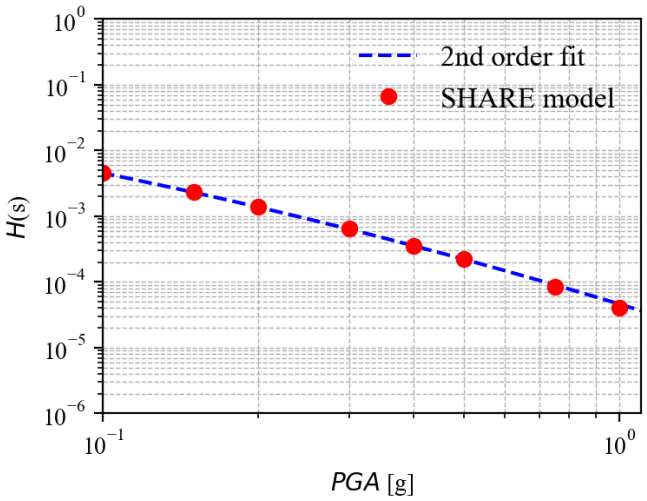

Figure 2: Second-order fit of a hazard curve for *PGA* at L'Aquila.

	OLS	SLS	ULS	Source
y	1%	25%	100%	User choice
T_R [years]	10	225	1600	User choice
H	1.00E-01	4.44E-03	6.25E-04	$=1/T_R$
β	0.1	0.2	0.3	Eurocode 8
λ	1.00E-01	4.65E-03	7.31E-04	Equation 2
EAL		0.64%		Equation 3
PGA [g]	0.01	0.10	0.28	Equation 1

Table 1: Design performance objectives defined by an ELR at each limit state, necessary to compute their respective MAFE and the design intensities.

Dispersions, β_s, were assumed based on those recommended in Appendix F of the recent draft of the revised Eurocode 8 [6] and are therefore deemed to be suitable for the present scope of illustration. In Figure 3, the EAL may be computed as the area beneath the approximate loss curve and is shaded in red. It is important to pay careful consideration since while the difference in area between the approximate and refined loss curve may appear insignificant, this is a result of the log scale of the vertical axis in Figure 3. However, it is possible to have an area between the two curves resulting in an EAL overestimation of up to 50% when compared to the refined curve. This can be overcome by using a closed-form expression with the same functional form of the refined loss curve as suggested by O'Reilly and Calvi [5]:

$$\lambda = c_0 \exp\left[-c_1 \ln y - c_2 \ln^2 y \right] \tag{3}$$

where the coefficients c_0, c_1 and c_2 can be fitted to pass through the three limit state points shown in Figure 3. The EAL was then evaluated as the area beneath this closed-form expression and is expected to be more representative of the actual EAL using more refined analysis. The ELR's were taken as y_{OLS}=1%, y_{SLS}=25% and y_{ULS}=100%, for the case study building. The values for the OLS and ULS limit states were based on the same consideration by O'Reilly and Calvi [5] whereby the OLS point is intended to represent the point at which the losses begin to accumulate and ULS when the losses reach the value of the building. The SLS point was chosen here and the sensitivity of the EAL to this value will be discussed in Section 4.1. The design EAL was established as the area under the refined curve, which was obtained as 0.64%, less than the target EAL (0.7%).

From each of these design limit state return periods, the design PGA was identified by inverting the hazard model in Equation 1 in terms of PGA. In the revised Eurocode 8, the 1600-year return period for the ULS corresponds to the significant damage limit state, so it was assumed to represent the complete replacement of the structure. In case of different design codes being used with differing minimum design requirements, such as NZS1170 or ASCE 7-16, the design return period of 2500 years is required at ULS, which may need to be accommodated as well.

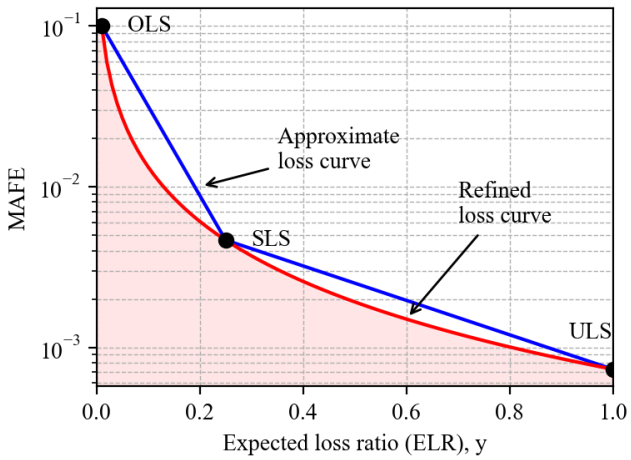

Figure 3: Approximate and refined loss curves, used to establish the design EAL shaded in red.

3.3 Identify structural design parameters

In order to convert the design loss ratios at both SLS and ULS into structural design parameters, storey loss functions (SLFs) were utilised and adopted from the literature [13]. Office occupancy was assumed and, for simplicity, only the typical SLFs were adopted (Figure 4). Considering the SLFs, the current formulation of CSD is not entirely compatible with their use when ELR is equal to 100% at ULS, since these functions' formulations tend to asymptotically increase towards large structural demand values of 15% storey drift (Figure 4), which are not realistic in design. To address this, a limiting value of 2% for PSD was adopted here, based on a sensitivity study presented in Section 4.2. Furthermore, some future developments to address this aspect relating to ULS performance are also envisaged in Section 4.3.

To link the ELR at each limit state to a structural demand parameter via the SLFs, as illustrated in Figure 4, the relative weights or contributions of the different component groups to expected loss, *Y*, were required. The ELR at each limit state is described by Equation 4:

$$y_{S,PSD} + y_{NS,PSD} + y_{NS,PFA} = y \tag{4}$$

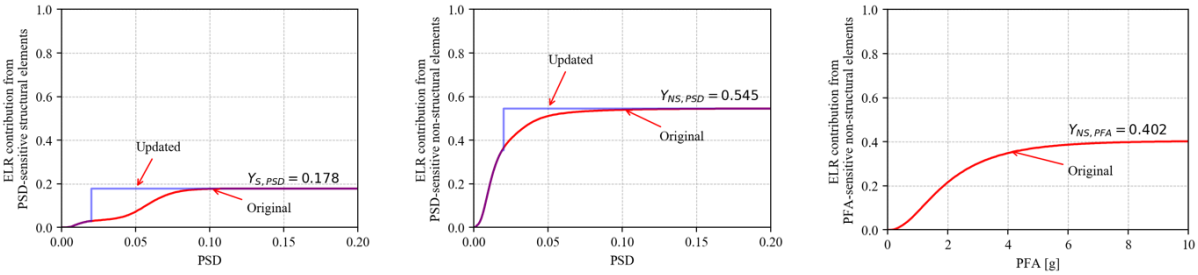

(a) PSD-sensitive structural elements

(b) PSD-sensitive non-structural elements

(c) PFA-sensitive non-structural elements

Figure 4: SLFs adopted from [13].

which is the sum of all sources of loss resulting from PSD-sensitive structural ($y_{S,PSD}$) and non-structural ($y_{NS,PSD}$) elements and PFA-sensitive non-structural ($y_{NS,PFA}$) loss contributions given in Figure 4. From Equation 4, the following expressions in Equation 5 can be written:

$$\begin{aligned} y_{S,PSD} &= yY_{S,PSD} \\ y_{NS,PSD} &= yY_{NS,PSD} \\ y_{NS,PFA} &= yY_{NS,PFA} \end{aligned} \tag{5}$$

meaning that the individual values of the damageable element group loss was computed as a product of the target ELR, y, and its relative weighting, Y, shown in Figure 4. By entering the vertical axis in Figure 4, these returned two values of θ_{max} and one value of a_{max} not to be exceeded in order to maintain that level of expected loss for that limit state. Taking the more critical of the two θ_{max} values at SLS, which will almost always be the non-structural-based value, the design demand parameters were established and are illustrated in Figure 5 and listed in Table 2.

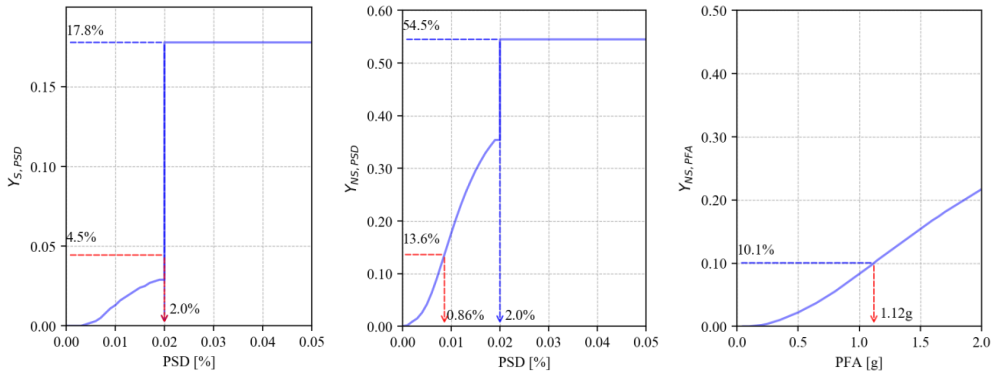

Figure 5: Illustration of the SLFs, and the identification of the design parameters for the SLS (red) and ULS (blue).

Structural demand parameter	SLS	ULS
PSD	0.86%	2.00%
PFA	1.12g	-

Table 2: Summary of structural design parameters for both limit states.

3.4 Compute spectral values

The identified values of θ_{max} and a_{max} at the SLS then needed to be converted to design spectral accelerations and displacements, $\Delta_{d,SLS}$ and α_{SLS}, respectively, as per Figure 1 (d). An equivalent single degree of freedom (SDOF) system is then employed in CSD to characterise a first-mode dominated multi-degree of freedom (MDOF) system. This is similar to the approach adopted in displacement based design (DDBD) [14] where the displacement of the equivalent SDOF system is given by Equations 6 and 7:

$$\Delta_d = \frac{\sum_{i=1}^{n} m_i \Delta_i^2}{\sum_{i=1}^{n} m_i \Delta_i} \tag{6}$$

$$\Delta_i = \omega_\theta \theta_{max} H_i \left(\frac{4H_n - H_i}{4H_n - H_1} \right) \tag{7}$$

where n is the number of storeys, m_i is the mass, Δ_i is the displaced shape at storey level i, ω_θ is the higher mode reduction factor and H_i is the i^{th} storey's elevation above the base. Detailed calculations are given in [5]. Unlike the PSD profile, PFA cannot be assumed to be first mode dominated, however, since the process of identifying a spectral acceleration, *Sa* for various building solutions assumes that the structure remains in the elastic range of response, some simplifications can be made. Combining the first few modes using square-root-sum-of-the-squares (SRSS) gives the PFA profile along the height, a_i, with a maximum value of a_{max}. For the case study building of RC frame with 4 storeys, the PFA may be approximated by a single coefficient γ defined as in Equation 8:

$$\alpha_{SLS} \approx \gamma a_{max} = 0.6 a_{max} \tag{8}$$

Initial parametric studies on the elastic modal properties of structures suggested that values of γ for low rise structures of 4 storeys of RC frame typology be around 0.6. Future research should look to improve this conversion, or at least refine this coefficient for different typologies of different number of storeys. For the purposes of CSD discussed here, they were deemed reasonable.

Table 3 lists the spectral acceleration and displacement for the case study building.

θ_{max} [%]	$\Delta_{d,SLS}$ [m]	a_{max} [g]	γ	α_{SLS} [g]
0.86	0.074	1.12	0.60	0.67

Table 3: Conversion of θ_{max} and a_{max} to spectral values at the SLS.

3.5 Quantify feasible initial secant to yield period range for SLS

The range of feasible initial secant to yield periods was identified using the equivalent SDOF spectral limits as presented in Table 3, which are illustrated in Figure 6, and the upper period bound, T_{upper}, for the RC frame in discussion was found to be 1.74 seconds. No lower period bound, T_{lower}, was identified, which is due to the fact that 0.67g of spectral acceleration is too high with respect to the maximum value of the spectrum at SLS (Figure 6). These bounds basically imply that the structure may be as stiff as needed since the SLS spectrum does not have enough spectral acceleration to exceed the PFA limits, while its flexibility will

be limited so that it does not undergo into excessive PSD. Hence, the period range is quite large, meaning that many potential design solutions could be accommodated. The damping was assumed as 5% for the case study RC frame.

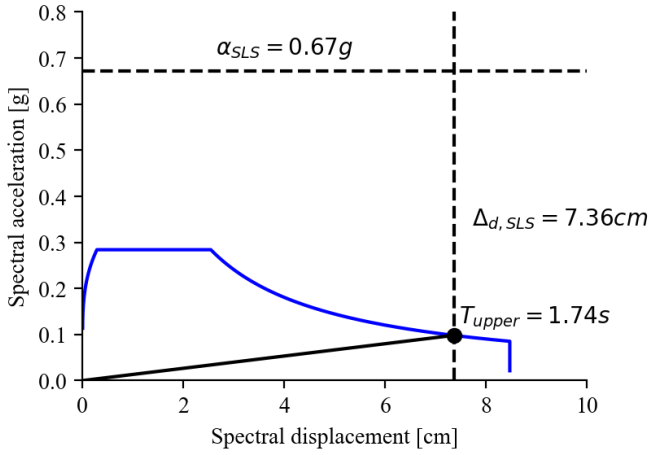

Figure 6: Identification of permissible initial secant to yield period range based on PFA and PSD limits for the SLS.

3.6 Establish required system strength and ductility

At the ULS, where the goal is to limit excessive PSD and provide a margin of safety against collapse during strong shaking, the effects of system non-linearity need to be accounted for. Figure 7 presents the permissible period range identified within the points 1 and 2, the trialled value of lateral strength capacity and the design solution space shaded in grey. It is important to note that for the case study building, point 2 is not representative since essentially there is no limit to the lower bound of the period range.

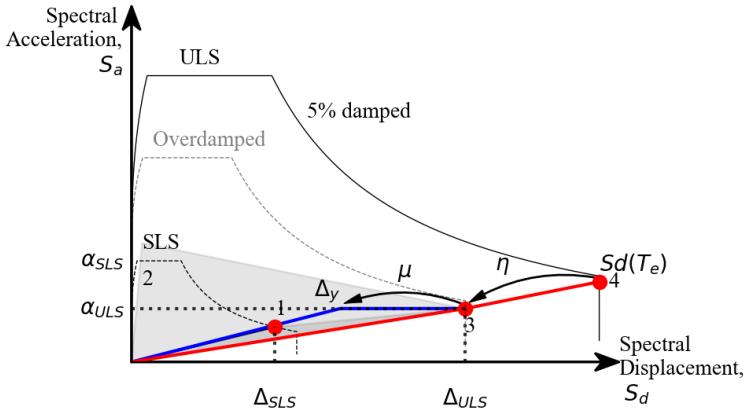

Figure 7: Identification of design solution space shaded in grey considering the permissible period range and the trialled value of lateral strength capacity (adapted from [5]).

For the given ULS spectrum and target design displacement, $\Delta_{d,ULS}$, a suitable SDOF system behaviour needed to be established. As noted by O'Reilly and Calvi [5], one way of doing this for the ULS, whilst still maintaining control over the initial period, is to simply trial a value of lateral strength. Then, by computing how much spectral reduction capacity would be required via non-linear behaviour, the structure's required ductility demand could be computed. This approach simply reworks the general DDBD approach, as the design displacement

and ULS spectrum are known but differs since the lateral strength is trialled and a compatible structural geometry is found (via the required yield displacement). DDBD, on the other hand, functions by commencing with a fixed structural geometry (meaning the yield displacement is known) and for the required ductility with respect to the design displacement and ULS spectrum, the lateral strength is found.

In this example, the approach described in [5] is followed but potential developments are described in Section 4.3. To account for the amplification in the structure's spectral capacity via non-linear behaviour of the structure, the effective period, T_e, passing from the origin through point 3 to point 4 was considered. In other words, the relation between linear and non-linear behaviour was found via a displacement modification factor (DMF) to the elastic design spectrum. As stated earlier, the design maximum PSD at ULS was 2.0% which gave a design displacement at ULS, $\Delta_{d,ULS}$, of 0.171m. Given $\Delta_{d,ULS}$ and the spectral displacement of the elastic response spectrum at T_e, $Sd(T_e)$, the required DMF, η, was determined from Equation 9.

$$\eta = \frac{\Delta_{d,ULS}}{Sd\left(T_e\right)} \tag{9}$$

Priestley *et al.* [14] outlined various expressions for different structural systems characterised by different hysteretic models representative of different structural systems and the one for RC frames was utilised here. From this relation, the required ductility, μ, was found by knowing the required spectral modification factor, η.

3.7 Compute structure backbone behaviour

With the knowledge of permissible period range, the design displacement, the lateral strength and the required structural ductility, the structure's backbone behaviour that respects these conditions was defined. The minimum required ductility already identified was then used to work back to find the yield displacement of the system, Δ_y, as per Equation 10.

$$\Delta_y = \frac{\Delta_{d,ULS}}{\mu} \tag{10}$$

The final bilinear backbone of the structural system was identified and is illustrated in Figure 8, where it was assumed that the second-order geometry effects, or P-Delta effects, were balanced out by the post-yield hardening of the structure to result in an elastic-perfectly plastic system.

The final values of yield displacement and lateral capacity are listed in Table 4. The base shear coefficient, *C*, is reasonable but the required initial period of the RC frame of 4 storeys is quite high to satisfy the design constraints. However, it is important to note that given a large range of allowable initial periods as identified earlier, a stiffer structure would have been obtained and this design scenario presented here was one of the many possibilities. This is a reflection of the current constraints imposed by the CSD at the ULS, where the advantage of being able to identify structural layouts is hampered by the fact that it tends to result in very flexible systems, as was the case in this example. Further consideration of the ULS performance that moves away from a single intensity-based verification of one PSD level (i.e. 2% PSD at 1600 years) should be pursued to arrive at a more risk-consistent approach to collapse safety. This would bring both CSD approach to a reasonable point whereby the losses via EAL and collapse safety are handled in a comprehensive manner. This was a limitation of CSD noted by O'Reilly and Calvi [5] and will be discussed further in Section 4.3

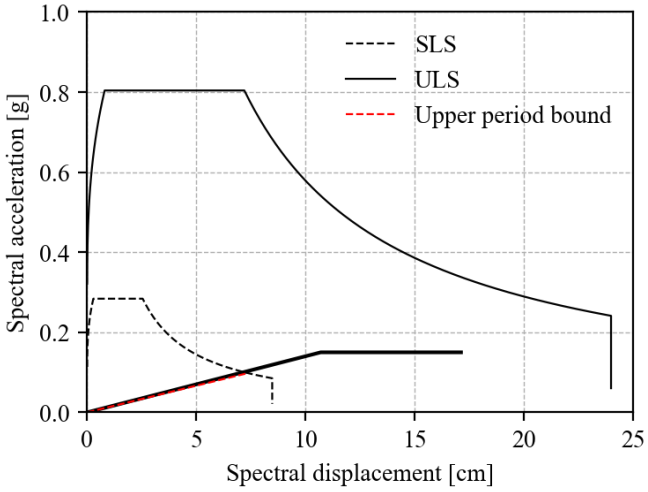

Figure 8: Required backbone response for the case study building design solution, where the period limits show how the design conditions have been respected.

a_{ULS} [g]	$\Delta_{d,ULS}$ [cm]	T_e [s]	$Sd(T_e)$ [cm]	$\eta_{required}$	Δ_y [cm]	$\mu_{provided}$	T_1 [s]	V_b [kN]	C
0.15	17.1	2.14	24.0	0.71	10.7	1.60	1.69	811	0.13

Table 4: Identification of structural system parameters to respect the design constraints, which fall within the design solution space

3.8 Identify structure layout

The final step of the design process was the identification of required geometry for the RC frame. In order to make use of the identified backbone leading to an acceptable building performance, defined in terms of expected loss, two parameters were required: the lateral strength and the yield displacement. As the lateral strength is a function of the member strengths, it can be easily adjusted by modifying the dissipative zone capacities. Structural geometry and material properties were required to establish the yield displacement. As the yield displacement was already known, the final dimensions and material properties of the structural system were identified as they are independent of the lateral strength [15].

For an RC frame with a ductile beam-sway mechanism, the yield drift, θ_y, has been shown by Priestley *et al.* [14] to be:

$$\theta_y = \frac{0.5\varepsilon_y B}{h_b} \tag{11}$$

where B is the bay width of the frame and h_b is the beam section height. Assuming a reinforcement of yield strength 350MPa and 200GPa of Young's modulus and a beam height of 0.5m, a bay width of around 6m would be required. Knowing the lateral load resisting system, structural geometry and the design base shear for the system, the structure can be detailed by providing enough capacity to ensure a ductile and stable mechanism. The resulting structural system would be representative of the backbone identified in Figure 8 and should satisfy the performance goals initially defined in terms of EAL described in Section 3.2.

4 DISCUSSION

Using the design framework summarised in Section 2 and implemented in a case study application in Section 3, additional studies on essential characteristics of the CSD framework were conducted. The goal was to understand whether the methodology could be improved in relation to the definition of the ULS performance and the sensitivity of the EAL to the SLFs. As before, the RC bare frame with office occupancy described in Section 3 was the reference design used for comparison throughout the discussion.

4.1 Influence of SLS parameters

One of the first studies regarding the definition of the performance objectives listed in Table 1 was on the sensitivity of the design EAL to the choices made regarding the return period of ground shaking, T_R, and the level of ELR at the SLS. The same values of y and T_R assumed for the OLS and ULS in Table 1 were maintained and the EAL was computed for numerous combinations of y_{SLS} and $T_{R,SLS}$. A summary of these design scenarios is presented in Figure 9. In essence, the hazard curve relates PGA (right axis) to T_R (left axis), and the SLF relates θ_{max} (top axis) to ELR (bottom axis). By increasing the y_{SLS} and $T_{R,SLS}$, the EAL, represented in green shades, will essentially stay constant. While, if the y_{SLS} is increased only or $T_{R,SLS}$ is decreased only, then the EAL will increase. Figure 9 then also shows the design solutions depending on $T_{R,SLS}$ and y_{SLS}. Only the upper bound results are shown, since the design indicated no lower period bound. The empty solution space represents an area where the solutions are beyond practicality, e.g. having high base shear coefficient, C, or high required bay width, B.

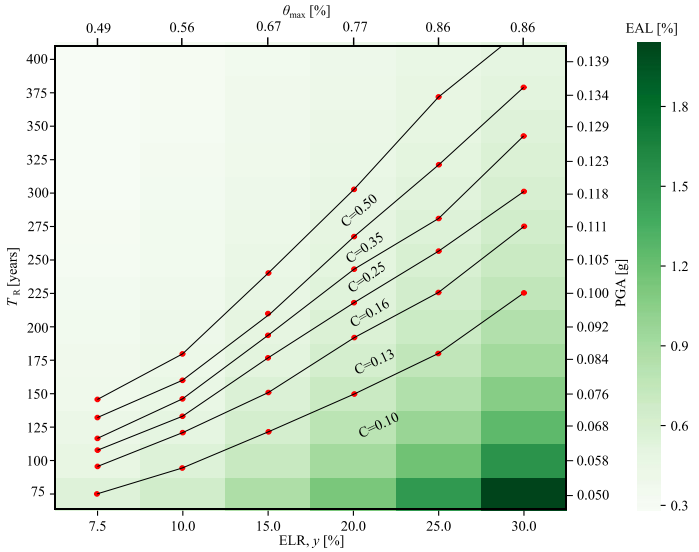

Figure 9: Impact of varying y_{SLS} and $T_{R,SLS}$ on the design EAL.

The study carried out on the variation of SLS parameters, showed high sensitivity of EAL to the SLS parameters. Additionally, the lower period range limit will be highly dependent on the *PGA* and subsequently $T_{R,SLS,}$ while the upper period range limit will be highly dependent on the θ_{max} and subsequently y_{SLS}. The curves defining C represent structures with an initial period equal to the upper period range limit and conditions imposed by each pair of $T_{R,SLS}$ and y_{SLS} below the curves can be satisfied by a structure with C equal to the curve value. Hence, the curves depend on an upper period range limit. Higher y_{SLS} and lower $T_{R,SLS}$ imply higher upper period range limit. For the study, the y_{SLS} was kept constant, while the $T_{R,SLS}$ was in-

creased sequentially, leading to a decreasing upper period range limit further constraining the design solution space, which resulted in the curves defining *C* boundaries.

4.2 Sensitivity study on SLFs

When using the SLFs as per Figure 4, the PSD at ULS for ELR=100% will be in the order of θ_{max}=10 to 20%. This value of θ_{max} may make sense purely from a monetary loss accumulation point of view, but is clearly unfeasible from a collapse performance perspective. To implement the CSD with these SLFs, a decision was made to limit θ_{max} to a certain limit similar to what ASCE 7-16 [8] prescribes to provide a level of life safety against collapse in their designs. This approach of utilising SLFs for the definition of the SLS design parameters but simply limiting the PSD to 2% at the ULS was adopted in the case study described in Section 3. The goal of the sensitivity study described here is to understand what impact this decision actually has on the design EAL. The SLF for PFA sensitive non-structural elements was not modified as the CSD methodology does not utilise the PFA at ULS.

Figure 10 shows the steps of the sensitivity study for the modification of SLFs for the CSD methodology. Initially, an original EAL was calculated through the employment of the SLF curves of the PSD-sensitive structural and non-structural elements adopted from Ramirez and Miranda [13]. Then a cut-off vertical line (in blue) representing a PSD value was gradually lowered, where the cut-off line describes a value of the PSD above which the ELR is assumed 100% times the respective weight of the element, Y_{PSD}. With each version of SLF, a corresponding EAL value was computed and then compared to the original one. The procedure was repeated until the error, ε_{EAL}, increased beyond 0.2% and the final updated SLF with the corresponding PSD cut-off line was used in the CSD presented herein.

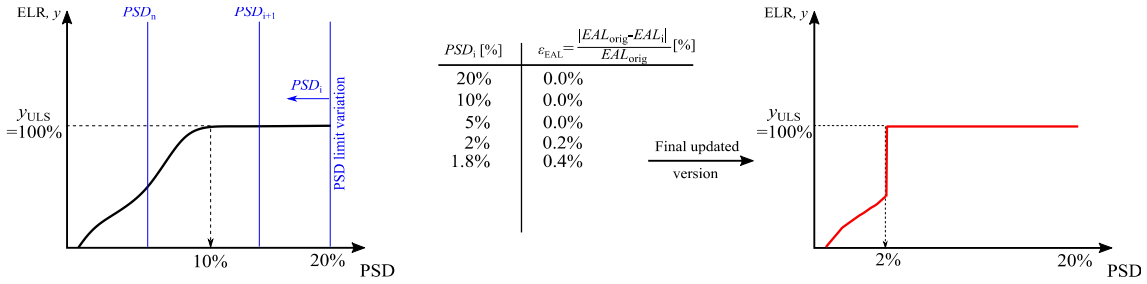

Figure 10: Sensitivity study on the modification of SLFs for the CSD methodology by the variation of PSD until EAL error, ε_{EAL}, is beyond 0.2%

The preliminary limit value obtained through the sensitivity study was 2% for PSD. By using the original and updated curves shown in Figure 4, the EAL variation error was found to be below 0.2%. Hence, the inclusion of such a limitation of PSD when utilising SLFs at ULS does not significantly impact the design EAL. Therefore, it can be concluded that the limitation of the PSD to 2% at ULS similar to what is done in the US with ASCE 7-16 [8], for example, with the aim for designing for collapse safety does not have any major impact on the design EAL that has been focused on up until now in CSD. Should the nature of determining the performance goals in CSD change from utilising EAL solely for the definition of the SLS limits and establishing an initial period range and then other possible criteria related to strength or ductility be utilised to protect against collapse, these two performance definitions will not have any major interaction with other and can be treated quite separately.

4.3 Consideration of collapse performance in design

As shown in the previous section, SLS and ULS performance can be handled with separate criteria without any major interference between them. With regards to collapse safety, MAFC, λ_c, may be used and a potential procedure to incorporate this in the CSD framework is described in Figure 11. The reasons for this are also illustrated in Figure 11(a) and are as follows. At ULS, a situation may occur where $\Delta_{d,ULS}$ is equal, or very close, to $Sd(T_e)$, meaning that the required DMF and consequently the ductility, μ, will be limited or equal to 1 (red point in Figure 11(a)). This will essentially result in designs with very long periods and limited ductility demand. Consequently, a high bay width will be required to provide a yield displacement equal to the required one. An alternative would be to neglect the condition of DMF equality, as also briefly discussed in O'Reilly and Calvi [5], and provide the structure with ductility higher than 1 (in blue in Figure 11(a)), which would then result in a lower bay width.

Alternatively, this could also be achieved by using MAFC to design for collapse safety in a more risk-consistent manner, as described a follows. An SDOF with period T that falls within the already identified period range [T_{lower}, T_{upper}] and an anticipated ductility capacity μ is considered. Knowing the yield lateral spectral acceleration, Sa_y, the dynamic performance of a trialled SDOF up to complete collapse can be quantified via SPO2IDA tool [16], as shown in Figure 11(b). Knowing the collapse fragility and the hazard curve, these may be integrated to get the MAFC, λ_c, where the collapse fragility defined in terms of R (Figure 11(b)) is transformed to spectral acceleration Sa by using a transformation factor, Γ, to a collapse fragility of the actual MDOF system (Figure 11(c)). By setting a target collapse safety to be respected by the resulting design, the base shear coefficient can be found for a given ductility, μ, and initial period, T_1. By varying T_1, a satisfactory base shear coefficient curve can be plotted in Sa versus Sd and the feasible structural solutions may be found (Figure 11(d)). It is noted that this approach is not too dissimilar to the yield frequency spectrum method [17] but here just the collapse behaviour is focused on, in addition to maintaining a degree of control on the EAL via the initial period range.

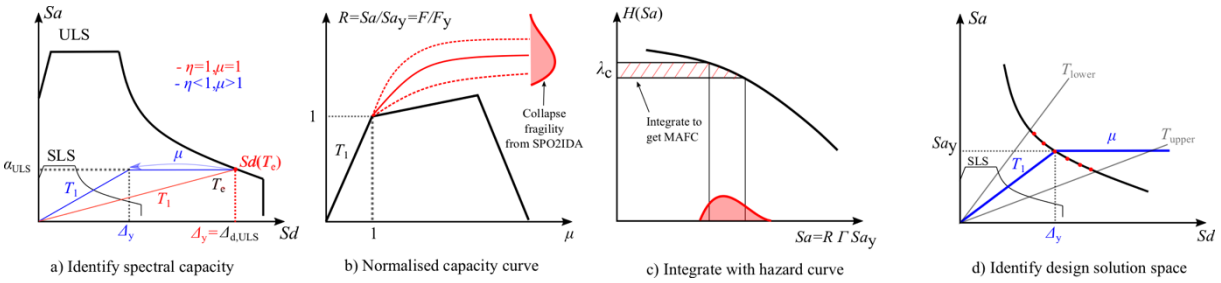

Figure 11: Potential development of the CSD framework to incorporate MAFC as a design variable.

The red dots in Figure 11(d) represent several of the numerous feasible design solutions within the period range that satisfy the collapse safety criterion. This approach would help to avoid the issue of SLFs identified in the previous section and overcome the difficulties explained in Section 3.6.

5 CONCLUSIONS

A novel CSD framework utilising EAL was used to identify feasible structural solutions aligning with the conceptual objectives of performance-based design. The general procedure with a case study application for an RC moment resisting frame was presented herein for its illustration. A number of assumptions were made: first, SLFs were used to convert ELRs to design PSD and PFA. At the ULS, where a collapse prevention requirement has to be met, the

PSD was cut-off at 2% and corresponds to the requirement brought forth by ASCE 7-16 [8]. Two limit state intensities, SLS and ULS, were utilised to characterise the structure's initial elastic and ductile non-linear behaviour. At SLS, design PSD and PFA were used to define a permissible initial secant to yield period range. Subsequently, with the choice of lateral strength and the knowledge of required system ductility, the yield displacement of the system was computed. Finally, the design solution space was identified and a potential bilinear backbone identified. Based on the characteristics identified, the required dimensions of the structure were identified as part of the first phase of design.

Moreover, some sensitivity studies were carried out to further investigate some particular aspects of the CSD framework. Several notes could be made based on these studies:

- High sensitivity of EAL and period range limits to the SLS parameters, as: 1) increasing ELR or decreasing T_R results in an increase of the EAL; and 2) decreasing T_R and increasing ELR will lead to an increase of the upper period range limit, meaning that care must be taken when establishing these points in design;
- Limiting PSD to 2% (similar to what is done in ASCE 7-16 with the aim to design for collapse safety) and modifying SLFs corresponded to an error in EAL of only 0.2%, demonstrating that it does not have any major impact on the design EAL;
- To avoid observed difficulties of implementing the CSD framework at ULS, an alternative approach was pondered. This does away with the issue where the required DMF and the ductility could potentially lead to large bay widths to satisfy the yield displacement requirement. The alternative approach foresees that the ULS is no longer considered, but rather a target MAFC, which is satisfied by a system with base shear coefficient, C, for a given ductility, μ, and an initial period, T, which must lie with the period range identified for SLS.

Within future developments, the CSD framework will be improved to include the current approach for SLS, where the elastic properties of the structure are chosen to satisfy the target EAL, while a simplified collapse analysis is used to satisfy a target MAFC.

6 ACKNOWLEDGEMENTS

The work presented in this paper has been developed within the framework of the project "Dipartimenti di Eccellenza", funded by the Italian Ministry of Education, University and Research at IUSS Pavia. The first author would like to acknowledge the financial support provided through the doctoral programme at IUSS Pavia.

REFERENCES

[1] Cornell CA, Krawinkler H. Progress and challenges in seismic performance assessment. PEER Cent News 2003:3(2): 1-2.

[2] SEAOC. Vision 2000: Performance-based seismic engineering of buildings 1995.

[3] Porter KA. An Overview of PEER's Performance-Based Earthquake Engineering Methodology. 9th Int Conf Appl Stat Probab Civ Eng 2003;273:973–80. doi:10.1.1.538.4550.

[4] Federal Emergency Management Agency. Seismic Performance Assessment of Buildings - methodology. Fema P-58-1 2012;1:278.

[5] O'Reilly GJ, Calvi GM. Conceptual seismic design in performance-based earthquake engineering. Earthq Eng Struct Dyn 2018:1–20. doi:10.1002/eqe.3141.

[6] EN 1998-1:2018. Design of structures for earthquake resistance (Draft) – Part 1: General rules, seismic actions and rules for buildings. Brussels: 2018.

[7] NZS 1170.5:2004. Structural design actions part 5: Earthquake actions. Wellington, New Zealand: 2004.

[8] ASCE 7-16. Minimum design loads for buildings and other structures. Reston, VA, USA: 2014. doi:10.1126/science.69.1782.217-a.

[9] Luco N, Ellingwood BR, Hamburger RO, Hooper JD, Kimball JK, Kircher CA. Risk-Targeted versus Current Seismic Design Maps for the Conterminous United States. Struct Eng Assoc Calif 2007 Conv Proc 2007:1–13.

[10] Vamvatsikos D. Performance-Based Seismic Design In Real Life : The Good, The Bad And The Ugly. Anidis 2017:17–24.

[11] Vamvatsikos D. Derivation of new SAC/FEMA performance evaluation solutions with second-order hazard approximation. Earthq Eng Struct Dyn 2013;42:1171–88. doi:10.1002/eqe.2265.

[12] Musson RW, Valensise G, Rovida AN, Woessner J, Cotton F, Hiemer S, et al. The 2013 European Seismic Hazard Model: key components and results. Bull Earthq Eng 2015;13:3553–96. doi:10.1007/s10518-015-9795-1.

[13] Ramirez CM, Miranda E. Building specific loss estimation methods & tools for simplified performance based earthquake engineering. 2009.

[14] Priestley MJN, Calvi GM, Kowalsky MJ. Displacement based seismic design of structures. Pavia, Italy: IUSS Press; 2007.

[15] Priestley MJN. Myths and Fallacies in Earthquake Engineering , Revisited. Pavia, Italy: IUSS Press; 2003.

[16] Vamvatsikos D, Cornell CA. Direct estimation of the seismic demand and capacity of MDOF systems through Incremental Dynamic Analysis of an SDOF approximation. J Struct Eng 2005;131:589–99.

[17] Vamvatsikos D, Aschheim MA. Performance-based seismic design via yield frequency spectra ‡. Earthq Eng Struct Dyn 2016;45:1759–78. doi:10.1002/eqe.2727.